Seeding of the nematic-isotropic phase transition by an electric field

MOTTRAM, N. J., CARE, C. M. and CLEAVER, D. J. <http://orcid.org/0000-0002-4278-0098>

Seeding of the nematic-isotropic phase transition by an electric field

N. J. Mottram, C. M. Care† and D. J. Cleaver†

Department of Mathematics,

University of Strathclyde,

Glasgow G1 1XH, UK.

†*Materials and Engineering Research Institute,*

Sheffield Hallam University,

Sheffield S1 1WB, UK.

Abstract

In this paper, we use a relatively simple continuum model to investigate the effects of dielectric inhomogeneity within confined liquid crystal cells. Specifically, we consider, in planar, cylindrical and spherical geometries, the stability of a nematic-isotropic interface subject to an applied voltage. Depending on the magnitude of this voltage, the temperature and the geometry of the cell, the nematic region may shrink until the material is completely isotropic within the cell, grow until the nematic phase fills the cell or, in certain geometries, coexist with the isotropic phase. For planar geometry, no coexistence is found, but we are able to give analytical expressions for the critical voltage for an electric-field-induced phase transition as well as the critical wetting layer thickness for arbitrary applied voltage. In cells with cylindrical and spherical geometries, however, stable nematic-isotropic coexistence is predicted, the thickness of the nematic region being controllable by alteration of the applied voltage.

I. INTRODUCTION

The nematic-isotropic (N-I) phase transition is weakly first order and so there exists a narrow temperature range over which the N and I phases coexist. In practice, however, for most systems the weakness of the N-I surface tension and the small enthalpy of the transition render experimental stabilisation of N-I coexistence a considerable challenge. Thus, most direct observations of the N-I interface have relied on imposition of a temperature gradient [1–3].

The conditions for N-I coexistence can also be influenced by the presence of disclinations, substrates or impurities, since such inhomogeneities can seed regions of one symmetry at state points for which the other is stable in 3d bulk. For example, order parameter variation at planar substrates has been observed in numerous experimental systems [4]. Indeed, there are a few cases where, by sandwiching a liquid crystal between substrates preferentially wet, respectively, by N and I phases, and imposing precise temperature control, thermally equilibrated N-I interfaces have been obtained [5, 6]. There are also numerous continuum and density functional treatments of liquid crystals adsorbed at substrates which show either partial or complete wetting by an I (N) film in the presence of a N (I) bulk [7, 8]. Correspondingly, substrate-induced order parameter variation is a common finding in computer simulation studies of confined and adsorbed liquid crystals [9, 10], leading to observation of phenomena such as capillary nematisation and criticality of the bulk N-I transition [11, 12].

A number of authors have also investigated the combined effects of applied bulk and surface fields on the N-I transition and wetting film growth [13, 14] although few analytical results have been reported. An applied orienting field can influence both surface and bulk order and may induce a transition to the N phase even when the I phase is the global minimiser of the bulk thermotropic energy. In practice, however, orienting fields are not applied directly; rather, they develop due to voltages applied across the dielectric liquid crystal contained in the device. As such, spatial inhomogeneity in the electric field (reflecting any dielectric inhomogeneity) is perfectly possible and certainly must occur in situations involving, e.g., an isotropic liquid crystal confined between substrates which induce significant orientational order in the interfacial regions. This situation is complicated even further in cells with very high resolution electrode patterns, where these inhomogeneities are two-dimensional [15].

In this paper we use a relatively simple continuum model to investigate the effect of dielectric inhomogeneity on the phase behaviour of a liquid crystals subject to an applied voltage. In particular, we examine the possibility of using an applied voltage to control the relative thicknesses of N and I domains by exploiting the dielectric differences between the two phases. We note that there is an analogy [16] to be drawn here with the shear-induced banding induced in colloidal liquid crystalline systems [17]. In these experiments, the system separates into N and I bands rather than adopting a continuous stress field across the entire shear cell [18]. Unlike these colloidal systems, however, the N-I interface in a single-component molecular system is characterised by a very small amplitude density step. Thus, unusually, the significant dielectric discontinuity seen at this interface has a very small associated compositional change. Consequently, formation of this particular phase boundary does not require substantial material transport.

The remainder of this paper is structured as follows. In the next two sections, we present the three geometries considered and detail, for each setup, the relevant contributions to the free energy of the system. In the subsequent section we give the resultant analysis for a planar-geometry cell. Following a description of the results obtained for this planar system, we then determine the corresponding results for systems with cylindrical and spherical geometries. Finally, the implications of these results are discussed.

II. GEOMETRIES

We consider liquid crystal systems with three different geometries: planar, cylindrical and spherical. In all three geometries we consider mesogenic material to be sandwiched between two substrates and hypothesise that, in the absence of an applied field, substrate-induced regions of N and I phases reside within this sandwich.

In the planar geometry the liquid crystal material is sandwiched between two flat parallel substrates (see Fig. 1(a)), one of which favours homeotropic alignment. It is assumed that a region with N order is induced at one of the substrates due to partial or complete wetting [7]. It is further assumed that electrodes are deposited on the inner surfaces of the substrates so that an electric field may be applied in the direction parallel to the substrate normal, the z direction. The substrates are a distance d apart and the N material occupies a region of thickness d^*, whilst the I phase fills the rest of the cell.

In the cylindrical and spherical geometries (see Figs 1(b) and (c)) the liquid crystal material fills the region between two concentric cylindrical or spherical shells, respectively. Here, electrodes are deposited on the inner face of the outer cylinder/sphere and the outer face of the inner cylinder/sphere. Any applied electric field, therefore, points in the radial direction. The radii of the inner and outer cylinder/sphere are R and $R+d$ and the nematic region, between $r = R$ and $r = R + d^*$, is taken to be adjacent to the inner cylinder/sphere.

III. FREE ENERGY

Our main concern in what follows is the effect of an applied voltage on the total thickness of the N region. Specifically, we consider whether the dielectric discontinuity associated with an N-I interface can be used to generate field-controllable domain thicknesses. To simplify the description of this system, we first assume that the nematic order parameter, S, is constant within each phase-region and that the interfaces between the N and I regions have a finite and constant surface tension.

With the substrate adjacent to the N region inducing homeotropic alignment, the electric field assumed to be aligned with the z-axis (in the planar case) or the local r-axis (in the cylindrical and spherical cases) and the liquid crystal chosen to have a positive dielectric anisotropy, the director within the N layer can be taken to lie along the z-axis (planar) or the radial direction (cylindrical, spherical). However, the electric field also induces an increase in order within both the N and I regions. In fact the I region becomes paranematic, that is a state with nematic symmetry about the field-axis but with a low order parameter. If we assume that the system remains uniaxial (a valid assumption since the homeotropically aligned surfaces do not induce biaxiality and, in this system, the dielectric effect of the field will tend to increase uniaxial order and reduce any biaxiality present) the liquid crystalline order can be described by the symmetric traceless tensor,

$$\mathbf{Q} = S(\mathbf{n} \otimes \mathbf{n} - \mathbf{I}/3)\,, \tag{1}$$

where $\mathbf{I}$ is the identity tensor. The product $\mathbf{n} \otimes \mathbf{n}$ produces the three by three matrix with ij^{th} entry equal to $\mathbf{n}_i\mathbf{n}_j$, the product of the i^{th} and j^{th} components of the director. The total free energy of the system, F, can then be expressed as the sum of: a thermotropic energy contribution, F_t, which describes the preference for the material to be in the N or I

phase; an elastic distortion energy F_d; an electrostatic energy contribution, F_e, which will be different in the paranematic and N regions due to the different permittivities of the phases; and an interfacial energy, F_i, for the N-I interface.

In the planar geometry case there will be no distortion of the director and the interfacial area will be unchanged as the N region changes size. Therefore, in the planar case, the elastic contribution to the free energy will be zero and the interfacial contribution will be constant (with respect to changes in d^*).

In general, the free energy is therefore

$$F = F_t + F_d + F_e + F_i = \int_{Vol} (\mathcal{F}_t + \mathcal{F}_d + \mathcal{F}_e)\, \mathrm{d}v + \int_A \mathcal{F}_i\, \mathrm{d}s \tag{2}$$

where, to recap, *Vol* is the volume occupied by the combined N and I regions, A is the area of the N-I interface and $\mathcal{F}$ denotes the appropriate free energy density contributions. Clearly, F is dependent on the order parameters within both the paranematic and N layers, S_I and S_N, respectively, and the total thickness of the N layer, d^*. Minimising F with respect to these three variables, therefore, offers a route to determining the equilibrium states for these systems.

A. Thermotropic energy

Following the classic Landau-De Gennes treatment [13], the thermotropic energy density of the nematic is approximated using a truncated Taylor expansion in the tensor order parameter,

$$\mathcal{F}_t = \mathcal{F}_0 + \frac{a}{2}\,\mathrm{tr}\left(\mathbf{Q}^2\right) + \frac{b}{3}\,\mathrm{tr}\left(\mathbf{Q}^3\right) + \frac{c}{4}\left(\mathrm{tr}\left(\mathbf{Q}^2\right)\right)^2 , \tag{3}$$

where $\mathcal{F}_0$ is the energy density of the I phase and tr denotes the trace operator. In principle, the coefficients a, b and c can all be temperature dependent although it is usual to assume that $a = \alpha\,(T - T^*)$ is linear in temperature T, while α, b and c are all constants. In this expression, T^* is the supercooling limit, the temperature at which the I phase becomes unstable.

Using the uniaxial expression for $\mathbf{Q}$ given in eq. (1) the thermotropic energy then becomes,

$$\mathcal{F}_t = \mathcal{F}_0 + \frac{\alpha}{3}\,(T - T^*)S^2 + \frac{2b}{27}\,S^3 + \frac{c}{9}\,S^4 = \mathcal{F}_0 + \sigma(S)\,, \tag{4}$$

where the shorthand notation $\sigma(S)$ will be used in later sections. The constant $\mathcal{F}_0$ will not enter the energy minimisation and will therefore be neglected in future expressions. There

are, at most, three extrema of this thermotropic energy expression, the I phase $S = 0$ and two N states $S_+ = (-b+\sqrt{b^2 - 24\,\alpha c(T - T^*)})/4c$ and $S_- = (-b-\sqrt{b^2 - 24\,\alpha c(T - T^*)})/4c$ (one stable and one unstable). There are also three significant temperatures: the temperature at which the I phase ceases to be metastable, the supercooling limit T^*; the temperature at which the energy density of the I phase $S = 0$ and the energy density of the N phase $S = S_+$ are equal, the clearing point, given by $T_{NI} = T^* + b^2/27ac$; and the temperature above which the N phase ceases to be metastable, the superheating limit given by $T^+ = T^* + b^2/24ac$. Within the temperature range $T < T^+$ the state $S = S_+$ is the relevant stable N state. With parameter values $\alpha = 1.5 \times 10^5$ J m^{-3} K^{-1}, $b = -2.25 \times 10^6$ J m^{-3} , $c = 4.5 \times 10^6$ J m^{-3} the superheating and clearing point are $T^+ = T^* + 0.3125$ K and $T_{NI} = T^* + 0.2778$ K.

B. Electrostatic energy

Assuming an absence of permanent dipoles or free charges, the electrostatic energy of the system is taken to derive from the dipoles induced when a voltage is applied across the cell. The electrostatic free energy density is then,

$$\mathcal{F}_e = -\int \mathbf{D}.\mathrm{d}\mathbf{E} = -\frac{1}{2}\epsilon_0(\boldsymbol{\epsilon}.\mathbf{E}).\mathbf{E}\,, \tag{5}$$

where $\mathbf{E}$ is the electric field, $\mathbf{D} = \epsilon_0\boldsymbol{\epsilon}\mathbf{E}$ is the displacement field, ϵ_0 is the permittivity of free space and $\boldsymbol{\epsilon}$ is the dielectric tensor.

Using Maxwell's equations, in the planar, cylindrical and spherical cases, for a charge-free system it is then relatively straightforward to show that the electric field in the substrate normal direction is

$$E_z(z) = \frac{1}{\epsilon_0\epsilon_{zz}(z)}\left(\frac{-V}{\int_0^d \frac{1}{\epsilon_0\epsilon_{zz}(z)}\mathrm{d}z}\right), \tag{6}$$

for the planar case,

$$E_r(r) = \frac{1}{\epsilon_0\epsilon_{rr}(r)}\frac{1}{r}\left(\frac{-V}{\int_R^{R+d} \frac{1}{\epsilon_0\epsilon_{rr}(r)}\frac{1}{r}\mathrm{d}r}\right), \tag{7}$$

for the cylindrical case, and

$$E_r(r) = \frac{1}{\epsilon_0\epsilon_{rr}(r)}\frac{1}{r^2}\left(\frac{-V}{\int_R^{R+d} \frac{1}{\epsilon_0\epsilon_{rr}(r)}\frac{1}{r^2}\mathrm{d}r}\right), \tag{8}$$

for the spherical case. Here V is the potential difference between the two substrates (with the higher voltage applied at the upper/outer surface) and $\epsilon_{zz}(z)$, $\epsilon_{rr}(r)$ are the zz and rr components of the dielectric tensor which may change through the cell.

Writing the dielectric tensor as

$$\boldsymbol{\epsilon} = \bar{\epsilon}\mathbf{I} + \Delta\epsilon^{*}\mathbf{Q}\,, \tag{9}$$

and assuming uniaxiality throughout the cell, eq. (1) with $\mathbf{n} = \mathbf{e}_z$ or $\mathbf{n} = \mathbf{e}_r$, depending on the geometry, then leads to

$$\epsilon_{zz} \quad \text{or} \quad \epsilon_{rr} = \bar{\epsilon} + \frac{2\Delta\epsilon^{*}S}{3}\,, \tag{10}$$

where $\bar{\epsilon} = (\epsilon_{||} + 2\epsilon_{\perp})/3$ is the permittivity of the I phase and $\Delta\epsilon^{*} = (\epsilon_{||} - \epsilon_{\perp})/S_{exp}$ is the dielectric anisotropy scaled by the order parameter at which the experimentally determined permittivity values were taken, S_{exp}. Denoting the order parameter in the N phase as S_N and that in the I/paranematic phase as S_I then gives, in the respective phase regions, $\epsilon_N = \bar{\epsilon} + 2\Delta\epsilon^{*}S_N/3$ and $\epsilon_I = \bar{\epsilon} + 2\Delta\epsilon^{*}S_I/3$.

In the three geometries we consider here, there are N and paranematic regions, with fixed permittivity tensors ϵ_N and ϵ_I, respectively. Because of the simplicity of the geometries considered, the free energy densities eq. (5) may then be written as

$$\mathcal{F}_e = -\frac{1}{2}\epsilon_0\epsilon_{zz}{E_z}^2\,, \quad \text{or} \quad -\frac{1}{2}\epsilon_0\epsilon_{rr}{E_r}^2\,, \tag{11}$$

for the planar and non-planar geometries, respectively. The forms of E_z, E_r, ϵ_{zz} and ϵ_{rr} are then given by eqs. (6)-(8) and eq. (10) so that the integrals needed to calculate the electrostatic energy in the different regions can be evaluated analytically.

C. Elastic energy

The elastic energy of the material is defined in both the N and paranematic region but a true I phase will not support equilibrium elastic distortion. We use the standard Frank energy density for an achiral N [19]

$$F_d = \frac{K_{11}}{2}\left(\nabla\mathbf{n}\right)^2 + \frac{K_{22}}{2}\left(\mathbf{n}.\nabla\times\mathbf{n}\right)^2 + \frac{K_{33}}{2}\left(\mathbf{n}\times\nabla\times\mathbf{n}\right)^2\,, \tag{12}$$

where the K_{ii} are the Frank elastic constants of splay twist and bend, respectively, and the K_{24} saddle-splay term has been neglected since we assume the director exhibits fixed homeotropic anchoring at the substrate and interface [19]. The elastic constants are dependent on the order parameter; thus $K_{ii} = S^2L_{ii}$ where the L_{ii} constants are, largely, temperature independent.

For the planar case, when $\mathbf{n} = \mathbf{e}_z$ there is no distortion and the elastic energy density is zero. However, for the cylindrical and spherical cases the director exhibits a splayed structure $\mathbf{n} = \mathbf{e}_r$ and the elastic energy density eq. (12) becomes

$$\mathcal{F}_d = \frac{L_{11} S^2}{2} \frac{1}{r^2}. \tag{13}$$

The elastic energy, in the cylindrical and spherical geometries, can therefore be calculated by integrating eq. (13) over the nematic and paranematic regions, where $S = S_N$ and $S = S_I$, respectively.

D. Interfacial energy

The interfacial energy density can be taken to be proportional to the square of the difference between the order parameters in the N and paranematic regions,

$$\mathcal{F}_i = \gamma (S_N - S_I)^2, \tag{14}$$

and therefore the interfacial energy is simply

$$F_i = \gamma A (S_N - S_I)^2 \tag{15}$$

where A is the area of the interface and γ is a surface tension parameter for the N-paranematic interface. In the planar geometry the interfacial area is simply $A = l_x l_y$, the area of the cell. In the cylindrical case $A = 2\pi(R + d^*) l_z$ where l_z is the extent of the cylinder in the z direction. In the spherical case the interface area is $A = 4\pi(R + d^*)^2$.

IV. PLANAR GEOMETRY

In the planar geometry shown in Fig. 1(a) the electric field expression in eq. (6) may be evaluated analytically by setting $\epsilon_{zz} = \epsilon_N$ in $0 < z < d^*$ and $\epsilon_{zz} = \epsilon_I$ in $d^* < z < d$. The electric fields within the N and I regions then become

$$\mathcal{F}_e^N = -\frac{\epsilon_0 \epsilon_I}{2} \frac{V^2 \epsilon_I \epsilon_N}{(d^*(\epsilon_I - \epsilon_N) + d\epsilon_N)^2}, \quad \mathcal{F}_e^I = -\frac{\epsilon_0 \epsilon_N}{2} \frac{V^2 \epsilon_I \epsilon_N}{(d^*(\epsilon_I - \epsilon_N) + d\epsilon_N)^2}. \tag{16}$$

Splitting the free energy in eq. (2) into the N and I regions and using the free energy densities in eqs. (4), (16) and (14) then gives

$$F = l_x l_y \left(\int_0^{d^*} \sigma(S_N) - \frac{\epsilon_0 \epsilon_I}{2} \frac{V^2 \epsilon_I \epsilon_N}{(d^*(\epsilon_I - \epsilon_N) + d\epsilon_N)^2} \, \mathrm{d}z \right.$$

$$+ \int_{d^*}^{d} \sigma(S_I) - \frac{\epsilon_0 \epsilon_N}{2} \frac{V^2 \epsilon_I \epsilon_N}{(d^*(\epsilon_I - \epsilon_N) + d\epsilon_N)^2} \, \mathrm{d}z + \gamma (S_N - S_I)^2 \Bigg) \,, \tag{17}$$

where l_x and l_y are the extents of cell in the x and y direction. Upon integration, eq. (17) leads to

$$F/(l_x l_y) = \left(d^* \left(\sigma(S_N) - \sigma(S_I)\right) + d\sigma(S_I)\right) - \frac{1}{2} \frac{\epsilon_0 \epsilon_I \epsilon_N \, V^2}{\left(d^*(\epsilon_I - \epsilon_N) + d\epsilon_N\right)} + \gamma (S_N - S_I)^2. \tag{18}$$

This energy has a singularity at $d^* = d\epsilon_N/(\epsilon_N - \epsilon_I)$ but, since the N phase is more ordered than the paranematic phase, we may assume that $0 < \epsilon_I < \epsilon_N$ so that the singularity occurs for the non-physical region, $d^* > d$. With the applied voltage set to zero, minimisation of this free energy expression leads to the expected solutions $S_I = 0$ and $S_N = S_+$. A second minimisation of the free energy with respect to d^* (within the constraint that $0 \leq d^* \leq d$) leads to the results $d^* = 0$ (i.e. no N region) if $\sigma(S_N) > \sigma(S_I)$, and $d^* = d$ (i.e. a fully N cell) if $\sigma(S_N) < \sigma(S_I)$.

When a voltage is applied to the cell, however, the minimisation becomes more complicated due to the dependence of ϵ_I and ϵ_N on S_I and S_N. Very little analytical progress can be made with the full description of this situation and the free energy must be minimised numerically (see below). However, if we assume that the applied voltage does not significantly alter the order parameter in either region then an approximate analytical solution *may* be found. Assuming that the dielectric contribution to the energy is small compared to the thermotropic contribution is equivalent to having,

$$\frac{\epsilon_0 \bar{\epsilon} V^2}{d} \ll d\beta \,, \tag{19}$$

where β is of the same order as the thermotropic Landau-de Gennes coefficients a, b, c. Since $\epsilon_0 = 8.854 \times 10^{12} \, \mathrm{F m^{-1}}$ and, typically, $d \sim 10^{-5} \, \mathrm{m}$, $\beta \sim 10^6 \, \mathrm{J \ m^{-3}}$, $\bar{\epsilon} \sim 10^1$ this is equivalent to $V \ll 10^3$ volts which is well above the voltages applied in typical devices. We can, therefore, be relatively confident in using $(\epsilon_0 \bar{\epsilon} V^2)/(d^2 \beta) = \delta$ as a small parameter. A perturbation analysis can then be carried out using the assumption that, when $\delta \ll 1$, the N and paranematic order parameters can be approximated by expansion series about the values $S_N = S_+$ and $S_I = 0$,

$$S_N \ = \ S_+ + \delta S_{N1} + O(\delta^2), \tag{20}$$

$$S_I \ = \ \delta S_{I1} + O(\delta^2), \tag{21}$$

Solutions for S_{N1} and S_{I1}, as well as higher order terms in the expansions, can readily be found analytically, although these expressions are lengthy and are not presented here. Using the resulting approximations from eqs. (20) and (21), substituted into the total energy, we then obtain the free energy as a function of d^* only.

To illustrate the predictions of this approach, we show, in Fig. 2, plots of the free energy as a function of domain size d^* for various voltages but for a fixed temperature $T = T^* + 0.28$ K, which is between $T^+ = T^* + 0.3125$ K and $T_{NI} = T^* + 0.2778$ K so that the N phase is metastable. Other parameter values are $\alpha = 1.5 \times 10^5$ J m^{-3} K^{-1}, $b = -2.25 \times 10^6$ J m^{-3} , $c = 4.5 \times 10^6$ J m^{-3}, $\epsilon_\perp = 4.2$, $\epsilon_{||} = 9.6$, $S_{exp} = 0.6$ (so that $\Delta\epsilon^* = 9$ and $\bar{\epsilon} = 6$), $\epsilon_0 = 8.854 \times 10^{-12}$ Fm^{-1} and $d = 1.0 \times 10^{-5}$ m. The shaded area, where $d^* < 0$ or $d^* > d$ is outside the range of physically achievable domain sizes and so can be disregarded.

Fig. 2 shows the energy plot resulting from a numerical minimisation of the full free energy expression eq. (18) with respect to S_I and S_N, as well as the analytical results obtained using both the perturbation solution (based on the expansions (20) and (21)) and the most basic free energy expression which assumes $S_I = 0$ and $S_N = S_+$. We note that it is not possible to differentiate between these three sets of plots, the percentage difference between the numerical solution and the approximate solutions being at most 0.05%. This means that not only is the perturbation expansion solution an excellent approximation to the numerical solution, but even the crude simplification $S_I = 0$, $S_N = S_+$ is also extremely accurate.

With the simplification $S_I = 0$, $S_N = S_+$ we may go further analytically. By differentiating the free energy eq. (18) with respect to d^* we find that there are stationary points of the energy at

$$d^*_{max} = \frac{d\epsilon_N}{(\epsilon_N - \epsilon_I)} - |V|\sqrt{\frac{\epsilon_0\epsilon_N\epsilon_I}{2\,(\epsilon_N - \epsilon_I)\,\sigma(S_+)}}\,, \tag{22}$$

$$d^*_{min} = \frac{d\epsilon_N}{(\epsilon_N - \epsilon_I)} + |V|\sqrt{\frac{\epsilon_0\epsilon_N\epsilon_I}{2\,(\epsilon_N - \epsilon_I)\,\sigma(S_+)}}\,, \tag{23}$$

where, as indicated by the subscripts, it is possible to show (by considering $\mathrm{d}^2\bar{F}/\mathrm{d}(d^*)^2$) that d^*_{max} is a maximum of the energy and d^*_{min} is a minimum of the energy. However, these maximum and minimum points only exist when $\sigma(S_+) > 0$, that is when $T > T_{NI}$. For physical significance, it is also necessary for the nematic phase to exist at least as a metastable state and, therefore, we must also have $T < T^+$. From eqs. (22) and (23) we

can also see that, since $\epsilon_N > \epsilon_I$, we obtain $d^*_{min} > d$ and, thus, the stable equilibrium case is never physically relevant for this system geometry. The value of d^* corresponding to an energy maximum, given by eq. (22), *is* physically relevant in some cases; these values are indicated by the open circles in Fig. 2. From these, we see that, for cases with a total N domain width smaller than d^*_{max}, the N domains will shrink to leave the cell filled with the I fluid whereas when the total N domain width is larger than d^*_{max} the N domain will grow and fill the cell.

The maximum point lies within the cell, that is $0 < d^* < d$, when,

$$V_{min} = d\sqrt{\frac{2\epsilon_I \sigma(S_+)}{\epsilon_0 \epsilon_N \left(\epsilon_N - \epsilon_I\right)}} < V < d\sqrt{\frac{2\epsilon_N \sigma(S_+)}{\epsilon_0 \epsilon_I \left(\epsilon_N - \epsilon_I\right)}} = V_{max}\,. \tag{24}$$

Therefore, for any fixed temperature between T_{N-I} and T^+, there exists a minimum voltage such that for $V < V_{min}$, even a substrate-induced domain of size $d^* = d$ (the full cell filled with N) will not be able to maintain the cell in the N phase. The energy curve in Fig. 2 with $V = 7.5\,\text{Volts}$ is such a situation where a N domain of any size will shrink to leave an I cell. There is also a corresponding maximum voltage V_{max} above which a surface domain of size $d^* = 0$ will be unstable with respect to the full phase transition of the cell from I to N. In such cases, N order will develop at all points in the cell and, therefore, the transition from N to I will be homogeneous and not domain driven. In other words, any applied voltage $V > V_{max}$ will lead to a homogeneous I-N transition.

The behaviour of this field-induced seeding is summarised in the phase diagram, Fig. 3. For temperatures between T_{N-I} and T^+ no field-induced I-N transition is possible for voltages $V < V_{min}$. At fixed T in this temperature range, however, a field-induced transition to the N phase, through domain growth, will be possible for voltages in the range $V_{min} < V < V_{max}$. The precise value of V needed to induce this domain-growth process will depend on the inherent domain size in the system. Thus, for substrates which are completely wetted by a N film (leading to large d^*), a voltage close to V_{min} will suffice, whereas partially wet substrates will require $V \lesssim V_{max}$. This raises an intriguing prospect for patterned surfaces, that this domain growth will directly project the degree of surface-induced order into the state adopted across the entire cell width. For applied voltages greater than $V_{max}(T)$ a homogeneous transition occurs in this temperature region. For temperatures greater than T^+ the N phase is not a stable state and, therefore, the field-induced transition is not possible, although, the orienting effect of the applied field will induce some paranematic order

within the fluid.

V. NON-PLANAR GEOMETRIES

In the analysis presented in the previous section, the substrates confining the liquid crystal were taken to be planar and parallel. In this geometry, it was found that the global minimum of the free energy always corresponds to either a fully N or a fully I cell. For certain narrow ranges of voltage and temperature, however, the state adopted by the system was found to be controlled, in part, by the extent of any substrate-induced ordered domain. Indeed, for temperatures between T_{N-I} and T^+, it was shown that discontinuous switching from fully-N to fully-I states could be induced by simply changing the applied voltage (see Fig. 3) but no stable equilibrium states were found involving an N-I interface.

As we shall now show, however, equivalent analysis performed for cells with a non-planar geometry *does* predict arrangements corresponding to field-stabilised N-I coexistence over the limited temperature range $T_{N-I} \leq T \leq T^+$. Specifically, we show that for cylindrical and spherical cells it is possible to find a range of cell dimensions and voltages for which the global free energy is minimised by a state which includes a N-I interface. This effect occurs because, in these geometries, the electric field cannot be uniform throughout space; hence, in some situations, the global free energy may be minimised if the region of the cell with the stronger electric field is N while the remainder of the cell remains I.

In a non-planar geometry there is a non-zero contribution to the free energy from distortions in the director field and the free energy of the N-I interface is also dependent upon the position of the interface. Despite these additional effects, and subject to the assumption that it is valid to ignore any change in the order parameter due to the splay deformation, it is found that for typical values of the material parameters, a field-banded arrangement with a N-I interface can be the stable state.

A. Cylindrical Case

If we consider a system with cylindrical geometry, with an inner cylinder of radius R and a concentric outer cylinder of radius $R+d$ (see Fig. 1(b)), we may follow similar arguments to those in the previous section to show that the contributions to the free energy contributions

are given by

$$\begin{aligned} F_t/l_z &= \pi\left[\sigma(S_I)(d-d^*)(d+d^*+2R)+\sigma(S_N)d^*(d^*+2R)\right] \\ F_e/l_z &= \frac{\pi V^2\varepsilon_0\varepsilon_N\varepsilon_I}{\varepsilon_I(\log(R)-\log(d^*+R))+\varepsilon_N(\ln(d^*+R)-\ln(d+R))} \\ F_d/l_z &= \pi L_{11}\left[S_I^2\{\ln(d+R)-\ln(d^*+R)\}-S_N^2\{\ln(R)-\ln(d^*+R)\}\right] \\ F_i/l_z &= 2\pi\gamma(d^*+R)(S_I-S_N)^2 \end{aligned} \tag{25}$$

where l_z is the extent of the cylinder in the z direction. Note, for consistency with the results presented in Section IV, that in the limit of large radius, the above expressions for F_t and F_e, scaled by the surface area of the inner sphere, asymptote to the corresponding terms in the equivalent planar geometry expression (eq. (18)); this result can be demonstrated analytically.

However, it is not possible to progress analytically with this set of equations. Resorting to numerical calculations, therefore, we plot, in Fig. 4, the free energy of this system per unit length in the z direction. Here, we have used the same temperature, cell thickness and material parameter values as those employed in our planar-geometry calculations with, additionally, $\gamma = 1.0\times10^{-5}\mathrm{Nm}^{-1}$ and $L_{11} = 1.0\times10^{-11}\mathrm{N}$.

These results show that for a large inner cylinder radius the behaviour is similar to that found for the planar case (Fig. 4(a)): a nematic region will either expand to fill the region if d^* is greater than some critical value, or the I layer will expand to fill the region if d^* is smaller than the critical value. However, when the radius R of the inner sphere is reduced, a significant range of applied voltages exists for which the free energy has a *minimum* for $0 < d^* < d$, *i.e.* there is a stable *N-I* interface between the inner and outer cylinders (Fig. 4(b)). Furthermore, other result sets (not shown here) indicate that if the radius of the outer conductor and the applied voltage are increased sufficiently, it is possible to achieve thick N layers. It must be emphasised, however, that such coexistence only occurs over the narrow temperature range for which both the N and I phases are either stable or metastable.

B. Spherical Case

If we now consider a system with spherical symmetry consisting of an inner conductor of radius R surrounded by a concentric outer sphere of radius $R+d$ (Fig. 1(c)) the free energy

contributions can be expressed as

$$\begin{aligned} F_t &= \frac{4}{3}\pi\left[\sigma(S_I)\left((R+d)^3-(R+d^*)^3\right)\right. \\ &\qquad \left. +\,\sigma(S_N)\left((R+d^*)^3-R^3\right)\right] \\ F_e &= -\frac{2\pi\varepsilon_0\varepsilon_N\varepsilon_I R(d+r)(d^*+R)V^2}{\varepsilon_I d^*(d+R)+\varepsilon_N R(d-d^*)} \\ F_d &= 8\pi L_{11} d^* S_N^2 \\ F_i &= 4\pi\gamma(d^*+R)^2(S_I-S_N)^2 \end{aligned} \tag{26}$$

It is again not possible to progress analytically with this set of equations. However, as in the cylindrical case, we may plot the total energy as a function of d^* by evaluating S_I and S_N in eqs. (26) by numerical minimisation. We may also use the simple assumption that $S_I = 0$ and $S_N = S_+$ to simplify the total energy; as shown above, this is an extremely good approximation to the full energy expression.

Using the same parameter values as those employed in the cylindrical case, we show, in Figs. 5(a) and (b), energy plots for a range of voltages and for $R = 50 \times 10^{-5}\,\mathrm{m}$ and $R = 5 \times 10^{-5}\,\mathrm{m}$, respectively. As in the cylindrical case, when the radius R of the inner sphere is reduced sufficiently, there is a significant range of applied voltages for which a stable *N-I* interface develops between the inner and outer spheres.

VI. CONCLUSIONS

Using a relatively simple model of the effect of an applied voltage on the I to N phase transition, we have investigated the stability of the *N-I* interface under the influence of various electric field patterns. In the case of a planar geometry system, we have found that the *N-I* interface cannot be stabilised by the effects of dielectric inhomogeneity alone. Here, though, we have been able to find analytic expressions for the critical domain size eq. (22) and critical voltage eq. (24) at which field-induced transitions occur. Thus, from eq. (22), we see that the critical domain size, d^*_{max}, is linearly proportional to the modulus of the applied voltage and its temperature dependence is of the form $-(T - T_{NI})^{-1/2}$ due to the temperature dependence of $\sigma(S_+)$. Therefore, as the temperature decreases towards T_{NI} the critical domain size decreases, eventually leading to a homogeneous transition where domains are not necessary to seed the transition. From the minimum and maximum critical voltages

in eq. (24) we find that $V_{min}/V_{max} = \epsilon_I/\epsilon_N$ so that for a weakly anisotropic materials, where $\epsilon_N \approx \epsilon_I$, the range of voltages which induce a domain driven phase transition will be small.

For the cylindrical and spherical geometries we have found that it *is* possible, for a range of cell dimensions and voltages, to generate a stable *N*-*I* interface in the interior of the liquid crystal region. Furthermore, we have shown that, by changing the applied voltage, the interface position can be controlled and, so, moved to any point in the cell.

This result suggests a generally applicable route to stabilising *N*-*I* interfaces which has no recourse to, e.g., material-specific surface treatments. Such direct access to the *N*-*I* interface should enable assessment of the various molecular theories relating to same. Furthermore, there is interest in being able to continuously vary liquid crystal film thicknesses in the sub-micron range. This is particularly of interest in hybrid aligned nematic films where elastic theory predicts qualitative changes in the Q-tensor profile as the film thickness is reduced [20] but experiment and simulation suggest structural effects neglected by continuum methods [21, 22].

Our findings may also have some technological application. Most obviously, our predictions for the cylindrical geometry lead directly to the concept of active optical fibres in which the radius of the refractive index step can be varied in time and/or distance along the fibre. As noted above, for single-component molecular mesogens, this controllable dielectric interface has little associated compositional change, making material transport a secondary consideration. Alternatively, liquid crystal mixtures or even polymeric mesogen systems could be used, so as to increase the available thermal range of *N*-*I* coexistence at the cost of significantly slower switching times.

ACKNOWLEDGEMENTS

NJM would like to thank the EPSRC for funding through an Advanced Research Fellowship.

---

[1] D. Langevin-Cruchon and M. A. Bouchiat, Mol. Cryst. Liq. Cryst. **22**, 317 (1973).

[2] S. Faetti and V. Palleschi, Phys. Rev. E **30**, 3241 (1984).

[3] D. Yelin, Y. Silberberga, Y. Barad and J. S. Patel, App. Phys. Lett. **74**, 3107 (1999).

[4] B. Jérôme, Rep. Prog. Phys. **54**, 391 (1991).

[5] H. Yokoyama, S. Kobayashi and H. Kamei, Mol. Cryst. Liq. Cryst. **129**, 109 (1985).

[6] D. Todorović-Marinić and J. T. Gleeson, Phys. Rev. E **54**, 5227 (1996).

[7] T. J. Sluckin and A. Poniewierski, in *Fluid Interfacial Phenomena*, edited by C. A. Croxton (Wiley, New York, 1986).

[8] A. Poniewierski, Liq. Cryst. **24**, 1369 (2000).

[9] G. D. Wall and D. J. Cleaver, Phys. Rev. E **56**, 4306 (1997).

[10] G. D. Wall and D. J. Cleaver, Mol. Phys. **101**, 1105 (2003).

[11] D. J. Cleaver and M. P. Allen, Mol. Phys. **80**, 253 (1993).

[12] M. Dijkstra, R. van Roij and R. Evans, Phys. Rev. E **63**, 051703 (2001).

[13] T. J. Sluckin and A. Poniewierski, Phys. Rev. Lett. **55**, 2907 (1985).

[14] I. Lelidis, Liq. Cryst. **25**, 531 (1998).

[15] R. James, F. A. Fernández, S. E. Day, M. Komarcevic and W. A. Crossland, Mol. Cryst. Liq. Cryst **422**, 479 (2004).

[16] G. Derfel, Liq. Cryst. **27**, 829 (1998).

[17] M. P. Lettinga and J. K. G. Dhont, J. Phys. Cond. Matt. **16**, S3929 (2004).

[18] P. D. Olmsted and C. -Y. D. Lu, Phys. Rev. E **60**, 4397 (1999).

[19] I. W. Stewart, *The Static and Dynamic Continuum Theory of Liquid Crystals: A Mathematical Introduction* (Taylor and Francis, 2003).

[20] A. Šarlah and S. Žumer, Phys. Rev. E **60**, 1821 (1999).

[21] B. Zappone, Ph. Richetti, R. Barberi, R. Bartolino and H. T. Nguyen, Phys. Rev. E **71**, 041703 (2005).

[22] D. J. Cleaver and P. I. C. Teixeira, Chem. Phys. Lett. **338**, 1 (2001).

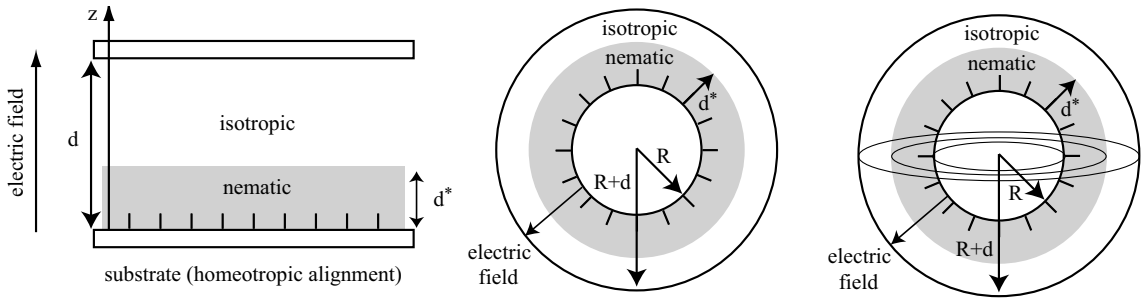

FIG. 1: Cell geometry: The liquid crystalline material is sandwiched between two planar, cylindrical or spherical substrates a distance d apart. The nematic layer, of thickness d^* is taken to occur close to the homeotropically anchored substrate.

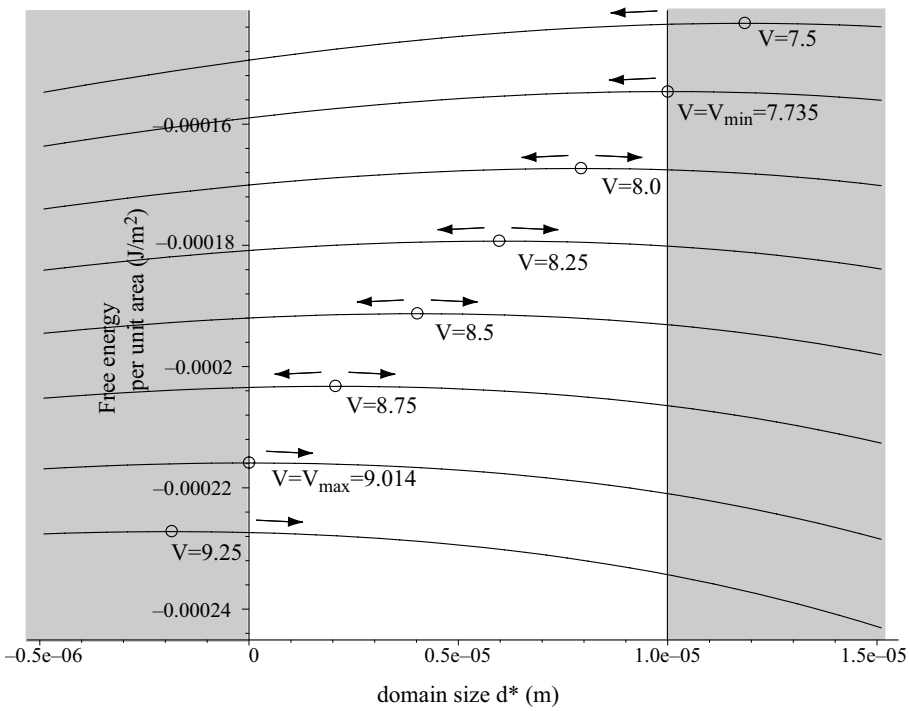

FIG. 2: The total free energy as a function of domain size d^* for voltages $V = 7.5$, $V_{min} = 7.735$, 8.0, 8.25, 8.5, 8.75, $V_{max} = 9.014$ and 9.25 Volts. As indicated by the arrows, for domain sizes less than the critical size (denoted by a circle for each voltage) where the maximum energy occurs, the system energy is reduced by shrinking the domain size to zero. For domains of size greater than the critical size, the system energy is reduced by growing the domain size to fill the cell. Three plots are shown for each parameter set (numerical solution of full problem and two analytical solutions to perturbation expansions - see text for details) but they cannot be resolved on the scale of this Figure.

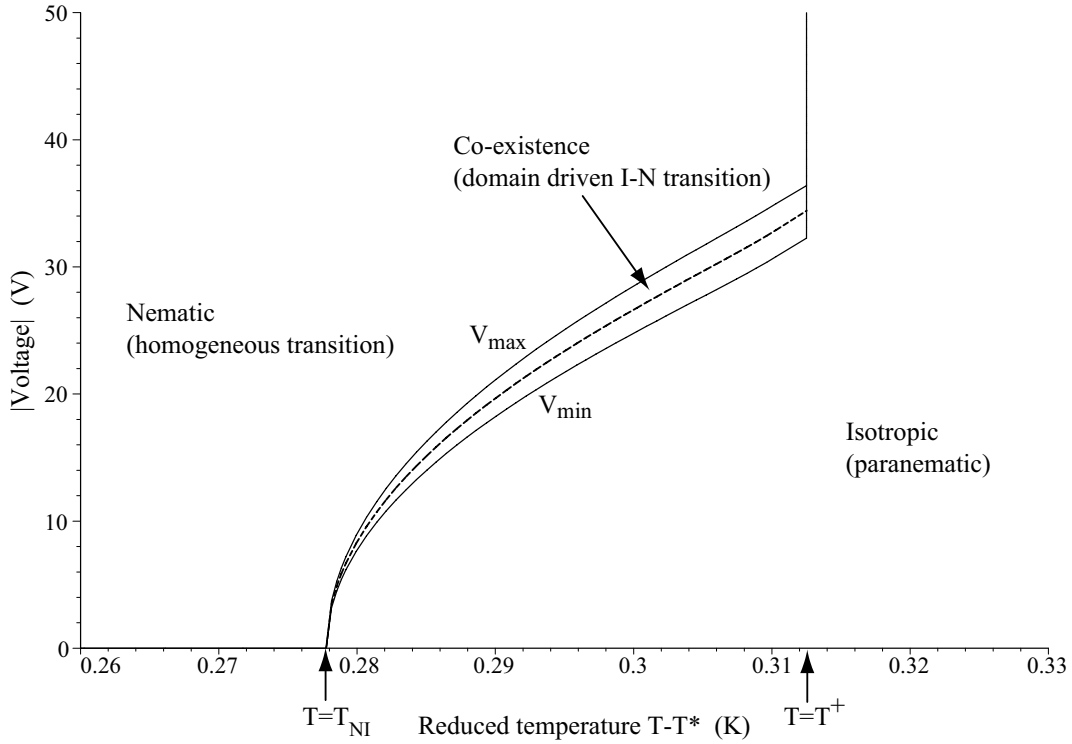

FIG. 3: The voltage-temperature phase diagram: there exists a region, between the curves V_{min} and V_{max}, where the stable state can be either fully nematic or fully isotropic, depending on the width of substrate-induced nematic domains present in the system. The critical size of the domain necessary depends on both T and V. For instance, along the dashed line a total nematic domain thickness corresponding to half of the cell width is necessary to induce a fully nematic state.

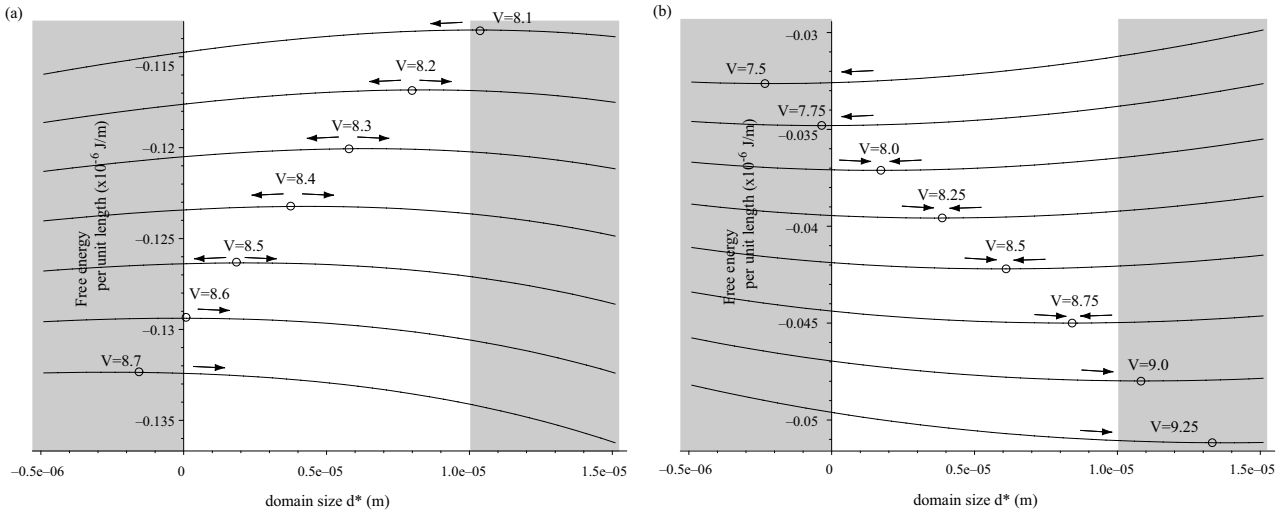

FIG. 4: The total free energy as a function of domain size d^* for (a) inner cylinder radius $R = 10 \times 10^{-5}$ m and voltages $V = 8$, 8.25, 8.5, 8.75 Volts (b) inner cylinder radius $R = 3 \times 10^{-5}$ m and voltages $V = 7.5$, 7.75, 8, 8.25, 8.5, 8.75, 9, 9.25 Volts. At small R, the free energy has a minimum within the cell, implying a coexistence or banding of the nematic and isotropic phases.

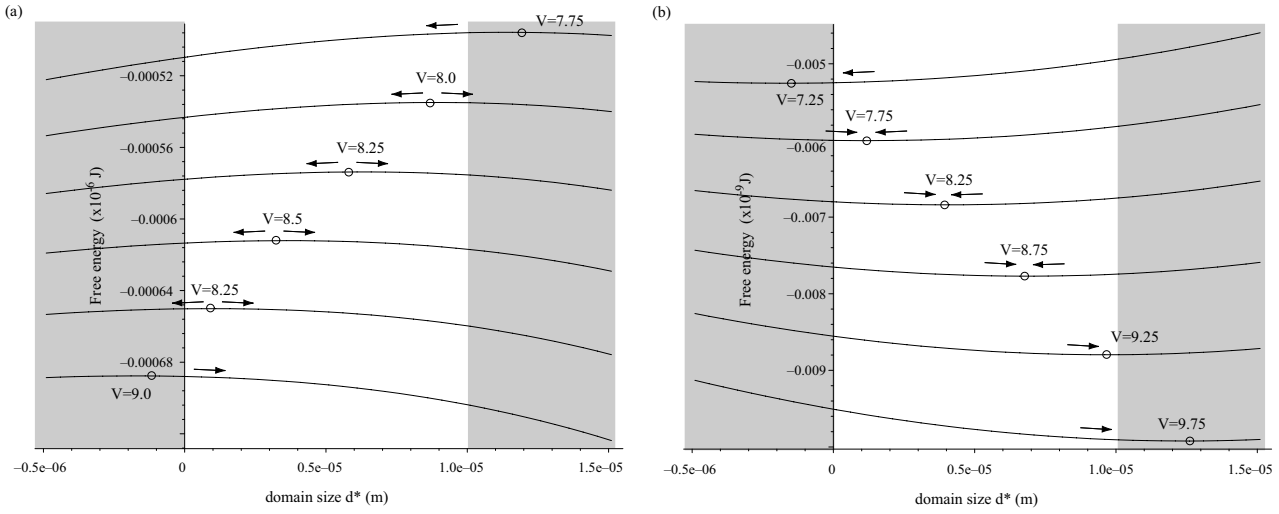

FIG. 5: The total free energy as a function of domain size d^* for (a) inner sphere radius $R = 50 \times 10^{-5}$ m and voltages $V = 7.75$, 8, 8.25, 8.5, 8.75, 9 Volts (b) inner sphere radius $R = 5 \times 10^{-5}$ m and voltages $V = 7.25$, 7.75, 8.25, 8.75, 9.25, 9.75 Volts. At small R, the free energy has a minimum within the cell, implying a coexistence or banding of the nematic and isotropic phases.